Energy Streamlines for Qualitative Inverse Scattering in Fluids and Solids

R. Aramini,[a)] G. Caviglia, and M. Piana

Dipartimento di Matematica,

Università di Genova,

via Dodecaneso 35,

16146 Genova,

Italy

(Dated: November 5, 2011)

Abstract

In time-harmonic acoustic fields, energy streamlines are defined as the integral curves of the power-flux density vector, averaged over a period. They provide a tool to visualize the details of propagation of energy. After reviewing the role of energy streamlines in the linear sampling method for acoustic inverse scattering, this work formulates a physical interpretation of the same qualitative method in the case of an isotropic homogeneous solid matrix. Specifically, it is shown that the linear sampling method results from conservation of energy along streamline tubes of energy flow associated with elastic waves.

PACS numbers: 43.60.Pt, 43.20.Bi, 43.20.Rz, 43.20.Gp, 43.40.Fz

I. INTRODUCTION

It is well known that the analysis of the energy streamlines of time-harmonic acoustic fields in fluids provides a method for displaying the properties of a given solution to the Helmholtz equation for the excess pressure[20,28]. An acoustic energy streamline is defined as a curve which is tangent at every point to the (time-averaged) vector of power-flux density $\mathbf{s}$, at that point. Unlike rays, energy streamlines do not represent alternative solutions or approximations to acoustic fields in a quiescent inviscid fluid. Rather, the acoustic field must be evaluated by solving the Helmholtz equation, before the corresponding power-flux density vector is determined and the related streamlines are traced as solutions to a system of ordinary differential equations[11,20].

Energy streamlines may be regarded as the paths along which energy is propagated by the acoustic field. Although complicated in some cases[28], these paths have been found of considerable interest from several viewpoints. They can give evidence to the involved details of energy flow in wave fields[14] (even in the case of discontinuous material parameters[11,21]), and may provide great practical advantages through applications in various problems of noise control in engineering[29].

Two recent papers[4,5] have given evidence to the role of energy streamlines in qualitative inverse scattering problems aiming at the determination of the unknown domain of an inhomogeneity immersed in a homogeneous and lossless background. In this case, the power-flux density vector $\mathbf{s}$ of the scattered field is divergence free, i.e.,

$$\nabla \cdot \mathbf{s} = 0 \quad \text{in} \quad \mathbb{R}^3 \setminus \bar{D}, \tag{1}$$

which implies a vanishing power flux across any closed surface formed by a tube of energy streamlines and two (non-intersecting) sections. Since the vector $\mathbf{s}$ is tangent to the walls of the streamline tube, there is no energy flow across the tube. Hence the power flux across the sections is conserved, as a direct manifestation of energy conservation[20]. If the flow tube

[a)]Electronic address: aramini@dima.unige.it

begins at the obstacle and goes to infinity, we can follow in detail the process of energy propagation by considering sections at increasing distance from the obstacle. Conversely, we can recover the flux at the boundary of the obstacle from the measured flux at infinity. This property is crucial for the interpretation of qualitative inverse scattering.

The linear sampling method[9] (LSM) is the most studied qualitative approach to inverse scattering. For scalar and time-harmonic fields, the LSM is based on the far-field equation

$$\int_{\Omega} u^s_\infty(\hat{\mathbf{x}};\mathbf{d}) g_{\mathbf{z}}(\mathbf{d})\, da_{\mathbf{d}} = \Phi_\infty(\hat{\mathbf{x}};\mathbf{z}), \tag{2}$$

where $\Omega = \{\mathbf{x} \in \mathbb{R}^3 : |\mathbf{x}| = 1\}$, $u^s_\infty(\hat{\mathbf{x}};\mathbf{d})$ is the far-field pattern of the scattered field in the observation direction $\hat{\mathbf{x}} \in \Omega$ for an incident plane wave propagating along $\mathbf{d} \in \Omega$, and $\Phi_\infty(\hat{\mathbf{x}};\mathbf{z})$ is the far-field pattern associated with the fundamental solution of the Helmholtz equation for a point source placed at $\mathbf{z}$. The general theorem at the basis of the LSM proves that there exists an approximate solution $g^\epsilon_{\mathbf{z}}$ of the far-field equation whose L^2-norm blows up when $\mathbf{z}$ approaches the scatterer's boundary and stays large when $\mathbf{z}$ is outside the scatterer. However, this same theorem is able to neither give a physical motivation of this behavior, nor explain the origin of the far-field equation in terms of fundamental theoretical description of the propagation and scattering processes. On the other hand, it has been proved for three-dimensional acoustic[4] and two-dimensional electromagnetic scattering[5] that a physical interpretation of the LSM is possible by establishing a link between the performance of the method and the conservation of energy through streamline tubes. In other terms, according to this mathematical physics viewpoint, the far-field equation can be interpreted as an energetic constraint on power fluxes associated with specific fields in the scattering process.

The aim of this paper is to formulate this same interpretation in the case of elastic scattering. As a first step, in section II we will review the connection between LSM and energy streamlines in the case of acoustic scattering. Then, in Section III, we will show that this link also holds in the case of (vector) solutions of the stationary Navier equation for waves in solids. Moreover, natural extensions and improvements of the LSM are proposed, suggested by this physical interpretation.

II. THE LSM IN ACOUSTIC INVERSE SCATTERING

Consider a three-dimensional (penetrable or impenetrable) scatterer occupying the open, C^2-domain D of boundary ∂D with outward unit normal $\mathbf{n}$. The obstacle is surrounded by a homogeneous, inviscid fluid at rest, of constant density ρ and sound speed $c > 0$. The LSM aims at determining, i.e., visualizing, the domain D through measurements of the scattered fields (far-field patterns) generated when incident time-harmonic plane waves hit the obstacle.

Denote by $\mathbf{x}$ the position vector in a suitable Cartesian orthogonal coordinate system and omit the harmonic factor $e^{-i\omega t}$, where ω is the constant angular frequency. The wavenumber in the background is then given by $k = \omega/c$, and the total acoustic pressure $p = p(\mathbf{x})$ satisfies the Helmholtz equation[17]

$$\Delta p + k^2 p = 0 \quad \text{in} \quad \mathbb{R}^3 \setminus \bar{D}, \tag{3}$$

while the velocity $\mathbf{v}$ is given in terms of p by $\mathbf{v} = \nabla p/(i\omega\rho)$.

Any pressure field p^s scattered by the obstacle and satisfying the Sommerfeld radiation condition may be represented as[17]

$$p^s(\mathbf{x}) = \int_{\partial D} \left[p^s(\mathbf{y}) \frac{\partial \Phi(\mathbf{x};\mathbf{y})}{\partial n} - \frac{\partial p^s(\mathbf{y})}{\partial n} \Phi(\mathbf{x};\mathbf{y}) \right] da_{\mathbf{y}}, \qquad \mathbf{x} \in \mathbb{R}^3 \setminus \bar{D}, \tag{4}$$

where

$$\Phi(\mathbf{x};\mathbf{z}) = \frac{e^{iks}}{4\pi s}, \qquad s = |\mathbf{x} - \mathbf{z}|, \tag{5}$$

denotes the fundamental solution generated by a unit source placed at $\mathbf{z}$: in other words, $\Phi(\cdot;\mathbf{z})$ is a radiating solution of the Helmholtz equation in $\mathbb{R}^3 \setminus \{\mathbf{z}\}$. Equation (4) shows that the scattered field is determined by its values and those of the related normal derivative at the surface ∂D of the obstacle. An analysis of the asymptotic properties of the scattered field by means of the integral representation (4) shows that[17]

$$p^s(\mathbf{x}) = \frac{e^{i\,k\,r}}{r} \left[p^s_\infty(\hat{\mathbf{x}}) + O\left(\frac{1}{r}\right) \right], \qquad r = |\mathbf{x}| \to \infty, \tag{6}$$

where $\hat{\mathbf{x}} = \mathbf{x}/r$. The far-field pattern $p^s_\infty(\hat{\mathbf{x}})$ of $p^s(\mathbf{x})$ is defined over the unit sphere $\Omega = \{\mathbf{x} \in \mathbb{R}^3 : |\mathbf{x}| = 1\}$ and depends on the values of p^s and its normal derivative at ∂D,

as follows from (4). Its explicit expression is not reported here since it is not relevant in the subsequent discussion. According to (6), the scattered field has the same asymptotic behaviour as an outgoing spherical wave with amplitude $p^s_\infty(\hat{\mathbf{x}})$ depending on the radial direction. In particular, it is found that the far-field pattern of the fundamental solution with source at $\mathbf{z}$ is given by[17] $\Phi_\infty(\hat{\mathbf{x}};\mathbf{z}) = e^{-ik\hat{\mathbf{x}}\cdot\mathbf{z}}/4\pi$.

Within the LSM, the domain of the scatterer is determined by the following procedure. Consider an incident harmonic plane wave of the form $p^i(\mathbf{x};\mathbf{d}) = e^{ik\mathbf{d}\cdot\mathbf{x}}$, where the unit vector $\mathbf{d} \in \Omega$ identifies the direction of propagation. Denote by $p^s(\mathbf{x};\mathbf{d})$ the corresponding scattered pressure field and by $p^s_\infty(\hat{\mathbf{x}};\mathbf{d})$ its far-field pattern. The scalar function $p^s_\infty(\hat{\mathbf{x}};\mathbf{d})$, which is defined over $\Omega \times \Omega$, is regarded as a given measured datum: note, in particular, that the unit sphere parameterizes both the observation and incidence directions.

Then, consider the equation at the basis of the LSM[9,18], i.e., the so-called 'far-field equation' (FFE): it is the *linear* integral equation

$$\int_\Omega p^s_\infty(\hat{\mathbf{x}};\mathbf{d})\; g_{\mathbf{z}}(\mathbf{d})\, da_{\mathbf{d}} = \Phi_\infty(\hat{\mathbf{x}};\mathbf{z}), \tag{7}$$

parameterized by the source point $\mathbf{z}$ of Φ and written for the unknown $g_{\mathbf{z}} \in L^2(\Omega)$, where $L^2(\Omega) = \{f : \Omega \to \mathbb{C} : \int_\Omega |f(\mathbf{d})|^2\, da_{\mathbf{d}} < \infty\}$. In general, the FFE cannot be solved[5,6,9] for $g_{\mathbf{z}}$: this reflects the fact that the FFE is not derived from physical laws (i.e., from the equations describing the wave propagation), but rather is imposed as a tool to compute an indicator function for the support of the scatterer, as we are going to see. Indeed, there always exist[6,9] solutions $g^\epsilon_{\mathbf{z}}$ to the approximate FFE

$$\left\| \int_\Omega p^s_\infty(\cdot;\mathbf{d})\, g^\epsilon_{\mathbf{z}}(\mathbf{d})\, da_{\mathbf{d}} - \Phi_\infty(\cdot;\mathbf{z}) \right\|_{L^2(\Omega)} \leq \epsilon \tag{8}$$

for any positive ϵ, where $\|\cdot\|_{L^2(\Omega)}$ denotes the L^2-norm. In practice, the ϵ-approximate solution $g^\epsilon_{\mathbf{z}}$ is obtained through a regularization procedure (typically, a Tikhonov method). It is found that $\|g^\epsilon_{\mathbf{z}}\|_{L^2(\Omega)} \to \infty$ as $\mathbf{z}$ tends to the boundary of D from inside, and that $\|g^\epsilon_{\mathbf{z}}\|_{L^2(\Omega)}$ can be made arbitrarily large for $\mathbf{z}$ outside[6,9].

In order to implement the LSM, the solution $g^\epsilon_{\mathbf{z}}$ is evaluated at the sampling points $\mathbf{z}$ of a grid containing the obstacle. The scatterer is then identified by the plot of $\|g^\epsilon_{\mathbf{z}}\|_{L^2(\Omega)}$ at

the sampling points in that $\|g_{\mathbf{z}}^{\epsilon}\|_{L^2(\Omega)}$ acts as an indicator function, taking small values for $\mathbf{z}$ inside D and large values for $\mathbf{z}$ outside. The LSM is applied without any *a priori* information about the interaction between incident wave and obstacle: e.g., the obstacle may be sound soft, sound hard or penetrable. A detailed description of the LSM algorithm, with numerical examples in various scattering conditions, can be found in several papers (see e.g.[8,15,16,18]).

However, owing to the lack of a physical justification for considering the FFE, it is unclear why such an algorithm should work at all[4–7]. In order to address this issue, it has been shown in two recent papers[4,5] that the LSM is strictly related to the conservation of the energy transported by the scattered field. We are now going to describe a simplified proof of why the LSM works, as a consequence of energy propagation from the obstacle to infinity along streamlines. In the next section, a similar procedure is then shown to hold for scattering in isotropic solid backgrounds.

In general, the instantaneous acoustic power-flux density of an acoustic field is defined as the product $\Re p\, \Re \mathbf{v}$, with the velocity $\mathbf{v} = \nabla p/(i\omega\rho)$. What we call the power-flux density vector $\mathbf{s}$ is the corresponding time-average (over a period), which is given by[11,20]

$$\mathbf{s} = \frac{1}{2}\,\Re\left(p\,\bar{\mathbf{v}}\right) = \frac{1}{2\,\omega\,\rho}\,\Im\left(\bar{p}\,\nabla p\right). \tag{9}$$

Here superposed bars, $\Re$ and $\Im$ denote the complex conjugate, the real, and the imaginary part, respectively. The energy streamlines of p are defined as solutions to the Cauchy problem

$$\frac{d\mathbf{x}(\tau)}{d\tau} = \mathbf{s}\left(\mathbf{x}(\tau)\right), \qquad \mathbf{x}(0) = \mathbf{x}_0, \tag{10}$$

where $\mathbf{x}_0$ is a point of the surrounding medium. In the present framework, we consider the vector $\mathbf{s}$ associated with the scattered field p^s in the exterior of D, for any incident field (such as the plane wave $p^i(\mathbf{x};\mathbf{d}) = e^{ik\mathbf{d}\cdot\mathbf{x}}$) that is an entire solution of the Helmholtz equation: since both the total field p and the incident field p^i solve such equation in $\mathbb{R}^3 \setminus \bar{D}$, the same is then true for the scattered field $p^s = p - p^i$. Moreover, we assume that there are no critical points $\mathbf{y}$ such that $\mathbf{s}(\mathbf{y}) = 0$.

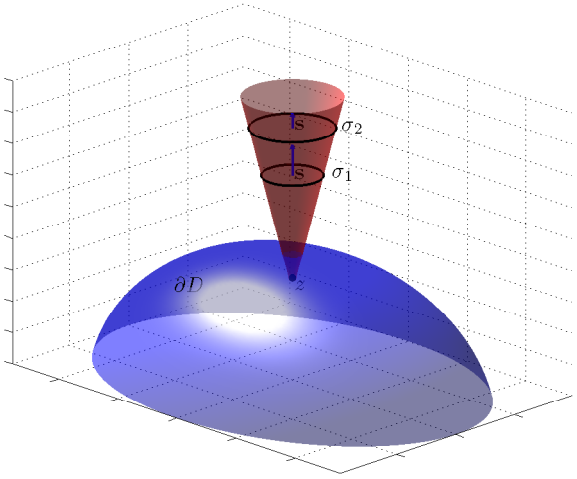

FIG. 1. Power flux through cross-sections of a flow tube formed by half-lines starting from a point $z \in D$.

If σ is any piecewise smooth surface with unit normal $\mathbf{n}$, then the integral

$$\mathcal{F}_\sigma[\mathbf{s}] := \int_\sigma \mathbf{s} \cdot \mathbf{n} \, da \tag{11}$$

yields the power flux through σ of the acoustic scattered field. For future purposes we recall a few properties of the power flux $\mathcal{F}_\sigma$.

From the Helmholtz equation and the definition (9) it follows that the power-flux density vector $\mathbf{s}$ is divergence free in $\mathbb{R}^3 \setminus \bar{D}$. Hence the vanishing of the corresponding flux across any closed surface that encloses no subset of D expresses conservation of energy. If the closed surface is identified with a portion of a flow tube delimited by non-intersecting surfaces σ_1 and σ_2 (see Fig. 1), then conservation of energy provides

$$\mathcal{F}_{\sigma_1}[\mathbf{s}] = \mathcal{F}_{\sigma_2}[\mathbf{s}] \tag{12}$$

if the normals are properly oriented. Equation (12) states the invariance of the power flux through cross-sections of a flow tube. If σ_1 is traced over the surface of the obstacle and if the flow lines "can reach infinity", the corresponding flow tube and the related cross-sections show how the power emanating from σ_1 is carried to infinity. If σ_1 coincides with the whole

boundary ∂D and σ_2 with the spherical surface Ω_r centred at the origin and of radius r large enough, then it follows from (6) and (12) that

$$\lim_{r\to\infty} \mathcal{F}_{\Omega_r}[\mathbf{s}] = \frac{k}{2\,\omega\,\rho}\,\|p^s_\infty\|^2_{L^2(\Omega)}\,. \tag{13}$$

Thus, the asymptotic power flux of the scattered field is proportional to the squared L^2-norm of the far-field pattern; in particular, it is positive. An equation of the form (13) holds if ∂D and Ω_r are replaced by cross sections of a flow tube, say, $\sigma_1 \subset \partial D$ and $\sigma_r \subset \Omega_r$, while Ω is replaced by $\tilde{\Omega} \subset \Omega$.

Next consider the pressure field

$$p^{s,\epsilon}_{\mathbf{z}}(\mathbf{x}) = \int_\Omega p^s(\mathbf{x};\mathbf{d})\, g^\epsilon_{\mathbf{z}}(\mathbf{d})\, da_{\mathbf{d}}, \quad \mathbf{x}\in\mathbb{R}^3\setminus D, \tag{14}$$

associated with a solution of the approximate FFE (8). The field $p^{s,\epsilon}_{\mathbf{z}}$ is generated by the superposition of incident plane waves with weight $g^\epsilon_{\mathbf{z}}$, i.e., by taking as incident field $p^{i,\epsilon}_{\mathbf{z}}(\mathbf{x}) = \int_\Omega e^{ik\mathbf{d}\cdot\mathbf{x}}\, g^\epsilon_{\mathbf{z}}(\mathbf{d})\, da_{\mathbf{d}}$, which is an entire solution of the Helmholtz equation[17]. The far-field pattern of $p^{s,\epsilon}_{\mathbf{z}}$ is approximately equal to the far-field pattern of the unit point-source at $\mathbf{z}$, since $g^\epsilon_{\mathbf{z}}$ solves (8). In general, this does not imply that the two fields $p^{s,\epsilon}_{\mathbf{z}}(\mathbf{x})$ and $\Phi(\mathbf{x};\mathbf{z})$ (and their energy streamlines) show the same features outside D, since the problem of determining a radiating field from its far-field pattern is ill-posed[17].

However, there are physical conditions (e.g., acoustic scattering by a sound-soft obstacle[4,6], or more generally, scattering by non-absorbing objects) whereby the regularization of the FFE allows a stable back-propagation of the restriction imposed by the FFE itself from the far-field region up to the boundary of the scatterer (if $\mathbf{z}\in D$). In this case, the scattered field $p^{s,\epsilon}_{\mathbf{z}}(\mathbf{x})$ can be made[4,6] arbitrarily close to the fundamental solution $\Phi(\mathbf{x};\mathbf{z})$ for $\mathbf{x}\in\partial D$. On the other hand,

$$\Phi(\mathbf{x};\mathbf{z}) = \frac{e^{ik|\mathbf{x}-\mathbf{z}|}}{4\pi|\mathbf{x}-\mathbf{z}|}, \tag{15}$$

and therefore $\Phi(\mathbf{x};\mathbf{z})$ diverges as $\mathbf{x}\to\mathbf{z}$: in particular, Φ diverges if $\mathbf{z}\in D$, $\mathbf{z}\to\mathbf{z}^*\in\partial D$, and $\mathbf{x}\to\mathbf{z}^*$. As a consequence, also $p^{s,\epsilon}_{\mathbf{z}}(\mathbf{x})$ diverges as $\mathbf{z},\mathbf{x}\to\mathbf{z}^*$. Because of (14) and the regularity of $p^s(\mathbf{x};\mathbf{d})$, this implies that $\|g^\epsilon_{\mathbf{z}}\|_{L^2(\Omega)}$ is unbounded as $\mathbf{z}\to\mathbf{z}^*$.

The stability of the back-propagation from the far-field to the near-field region has not been proved for generic scattering conditions, which means that the difference $p_{\mathbf{z}}^{s,\epsilon}(\mathbf{x}) - \Phi(\mathbf{x};\mathbf{z})$ is not necessarily small in the neighbourhood of the obstacle, and then the previous argument does not apply. However, as we are going to see, a weaker and more general assumption concerning the similarity of the streamlines of $p_{\mathbf{z}}^{s,\epsilon}(\mathbf{x})$ and $\Phi(\mathbf{x};\mathbf{z})$ for $\mathbf{z} \in D$ and $\mathbf{x} \in \mathbb{R}^3 \setminus D$ suffices to prove the unboundedness of $\|g_{\mathbf{z}}^{\epsilon}\|_{L^2(\Omega)}$ as $\mathbf{z} \to \mathbf{z}^*$, owing to energy conservation along the flow tubes of $p_{\mathbf{z}}^{s,\epsilon}(\mathbf{x})$. This assumption is rather natural if $p_{\mathbf{z}}^{s,\epsilon}(\mathbf{x}) \approx \Phi(\mathbf{x};\mathbf{z})$ for $\mathbf{x} \in \partial D$: indeed, the direct scattering problem is well-posed and then the approximate equality of two radiating fields on ∂D entails their approximate equality also outside D. Interestingly, numerical simulations suggest[3–5] that the streamlines of $p_{\mathbf{z}}^{s,\epsilon}(\mathbf{x})$ are approximately radial even when the condition $p_{\mathbf{z}}^{s,\epsilon}(\mathbf{x}) \approx \Phi(\mathbf{x};\mathbf{z})$ does not need to hold true (e.g., when lossy scatterers and/or backgrounds are considered, or aspect-limited measurements are used as input data for the LSM).

Then, to simplify the present discussion of the LSM and to give evidence to the underlying physics, we consider sampling points inside D and we assume that the energy streamlines of the fields $p_{\mathbf{z}}^{s,\epsilon}$ and $\Phi(\mathbf{x};\mathbf{z})$ coincide in the exterior of D. We refer to the cited papers[3–5] for mathematical details and for the case $\mathbf{z} \notin D$.

Therefore, let $\mathbf{z} \in D$. The energy streamlines of $\Phi(\mathbf{x};\mathbf{z})$ form a star-shaped family of half-lines outgoing from the singular point $\mathbf{z}$. For $\mathbf{z}$ close to the limit point $\mathbf{z}^* \in \partial D$, consider the spherical surface $\Omega(\mathbf{z}, r^*)$, of radius $r^* = 2\,|\mathbf{z} - \mathbf{z}^*|$ and center $\mathbf{z}$, and denote by $\Omega_{r^*}^*$ the portion of $\Omega(\mathbf{z}, r^*)$ external to D. Let Ω_r^* the part of the spherical surface $\Omega(\mathbf{z}, r)$ intersected by the energy streamlines outgoing from points of $\Omega_{r^*}^*$: a plane section of this geometric construction is shown in Fig. 2. The surfaces $\Omega_{r^*}^*$ and Ω_r^* intersect the same flow tube of $\Phi(\mathbf{x};\mathbf{z})$ outside D, so that we have

$$\mathcal{F}_{\Omega_{r^*}^*}[\mathbf{s}] = \mathcal{F}_{\Omega_r^*}[\mathbf{s}] > 0 \quad \text{as} \quad r \to \infty \tag{16}$$

because of (12) and (13). Eq. (16) also holds for the power-flux density vector associated with the pressure $p_{\mathbf{z}}^{s,\epsilon}$. As $\mathbf{z} \to \mathbf{z}^*$ the area of the surface $\Omega_{r^*}^*$ tends to 0 as the squared

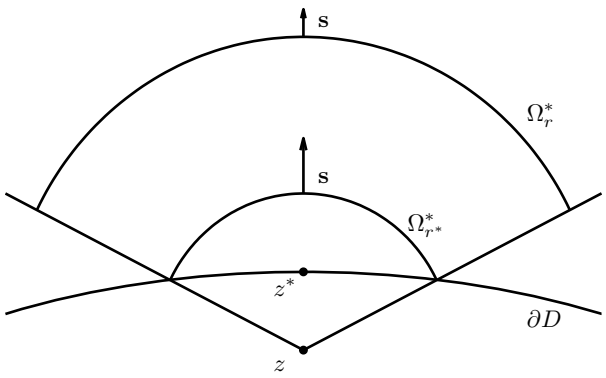

FIG. 2. Plane section of the geometric construction considered for eq. (16).

radius while the flux remains strictly positive because it equals the asymptotic flux of the flow tube formed by diverging streamlines. In view of (9), (11) and (14), this is only possible if $\|g_{\mathbf{z}}^{\epsilon}\|_{L^2(\Omega)}$ diverges as $\mathbf{z} \to \mathbf{z}^*$. Indeed, if $\|g_{\mathbf{z}}^{\epsilon}\|_{L^2(\Omega)}$ is bounded, then also $|p_{\mathbf{z}}^{s,\epsilon}|$ and $|\partial p_{\mathbf{z}}^{s,\epsilon}/\partial n|$ are bounded on $\Omega_{r^*}^*$, and the flux through $\Omega_{r^*}^*$ tends to zero.

Conservation of power flux through sections of a flow tube and positivity of the flux at infinity constitute the basic tools of this approach. However, in general, the energy streamlines of $p_{\mathbf{z}}^{s,\epsilon}(\mathbf{x})$ do not coincide with those of the fundamental solution $\Phi(\mathbf{x};\mathbf{z})$. Hence appropriate assumptions, supported by numerical simulations, are needed to ensure asymptotic properties resembling those of the streamlines of Φ.

III. ENERGY STREAMLINES AND THE LSM IN A SOLID BACKGROUND

The previous qualitative approach to inverse scattering problems may be extended to the more general framework of an obstacle surrounded by a linear, homogeneous, isotropic, elastic solid matrix, where a limited number of analytical results are known and refer to rather special cases[2,12,13,25,26]. The solid matrix is characterized by Lamé constants λ and μ, and mass density ρ. It is assumed that the strong ellipticity conditions $\mu > 0$ and $\lambda + 2\,\mu > 0$ are satisfied, so that the medium propagates both longitudinal and transverse waves[24].

The displacement of the particle $\mathbf{x}$ at the time t is denoted by $\mathbf{u}(\mathbf{x})\, e^{-i\,\omega\, t}$ and the time-

harmonic factor is again omitted. A displacement field $\mathbf{u}^s$ scattered by the obstacle obeys the (stationary) Navier equation

$$(\lambda+\mu)\,\nabla\,(\nabla\cdot\mathbf{u}^s)+\mu\,\Delta\mathbf{u}^s+\rho\,\omega^2\,\mathbf{u}^s=0, \tag{17}$$

inside the solid background, in the absence of sources. Then the radiation condition implies that $\mathbf{u}^s$ may be represented as[10,19,23]

$$\mathbf{u}^s(\mathbf{x})=\int_{\partial D}\{\boldsymbol{\tau}[\mathbf{G}]\cdot\mathbf{u}^s-\mathbf{G}\,\mathbf{t}^s\}\;da_{\mathbf{y}}, \tag{18}$$

where $\mathbf{x}$ is external to D. Here $\mathbf{G}(\mathbf{x};\mathbf{y})$ is the fundamental solution defined by

$$\mathbf{G}(\mathbf{x};\mathbf{y})=\frac{1}{\rho\,\omega^2}\,\left[k_s^2\,\Phi_s\,\mathbf{I}-\nabla\otimes\nabla\,(\Phi_p-\Phi_s)\right], \tag{19}$$

where $\mathbf{I}$ is the identity matrix and

$$\Phi_{p,s}(\mathbf{x};\mathbf{y})=\frac{e^{i\,k_{p,s}|\mathbf{x}-\mathbf{y}|}}{4\,\pi|\mathbf{x}-\mathbf{y}|};$$

the constant wavenumbers $k_{p,s}$ are defined by

$$k_p^2=\frac{\omega^2\,\rho}{\lambda+2\,\mu},\qquad k_s^2=\frac{\omega^2\,\rho}{\mu}.$$

The operator $\boldsymbol{\tau}[\cdot]$ evaluates the surface traction associated with the displacement inside square brackets. Accordingly we have

$$\boldsymbol{\tau}[\mathbf{G}]=\left[\lambda\;(\nabla\cdot\mathbf{G})\;\mathbf{I}+\mu\;\left(\nabla\mathbf{G}+(\nabla\mathbf{G})^T\right)\right]\mathbf{n},$$

and we have set $\mathbf{t}^s=\boldsymbol{\tau}[\mathbf{u}^s]$ in (18) to simplify. We conclude that Eq. (18) expresses $\mathbf{u}^s(\mathbf{x})$ for $\mathbf{x}\notin D$ in terms of $\mathbf{u}^s$ and $\mathbf{t}^s$ at ∂D.

Substitution of (19) into (18) provides the asymptotic expression of $\mathbf{u}^s$ in the form

$$\mathbf{u}^s(\mathbf{x})=\frac{e^{i\,k_p\,r}}{r}\left[\mathbf{u}^s_{p,\infty}\,(\hat{\mathbf{x}})+O\left(\frac{1}{r}\right)\right]+\frac{e^{i\,k_s\,r}}{r}\left[\mathbf{u}^s_{s,\infty}\,(\hat{\mathbf{x}})+O\left(\frac{1}{r}\right)\right]\quad\text{as } r\to\infty. \tag{20}$$

The vector $\mathbf{u}^s_{p,\infty}(\hat{\mathbf{x}})$, which is defined by

$$\mathbf{u}^s_{p,\infty}(\hat{\mathbf{x}})=-\frac{k_p^2}{4\,\pi\,\rho\,\omega^2}\,\hat{\mathbf{x}}\int_{\partial D}\{i\,\lambda\,k_p\,(\mathbf{u}^s\cdot\mathbf{n})+2\,i\,\mu\,k_p\,(\mathbf{u}^s\cdot\hat{\mathbf{x}})\,(\mathbf{n}\cdot\hat{\mathbf{x}})+(\mathbf{t}^s\cdot\hat{\mathbf{x}})\}\,e^{-i\,k_p\,\hat{\mathbf{x}}\cdot\mathbf{y}}\,da_{\mathbf{y}},$$

is radial, with intensity given by an integral over ∂D depending on the radial direction $\hat{\mathbf{x}}$ and on $\mathbf{u}^s$, $\mathbf{t}^s$ at ∂D. The vector $\mathbf{u}^s_{s,\infty}(\hat{\mathbf{x}})$ is given by

$$\mathbf{u}^s_{s,\infty}(\hat{\mathbf{x}}) = \hat{\mathbf{x}} \wedge [\mathbf{U}_{s,\infty}(\hat{\mathbf{x}}) \wedge \hat{\mathbf{x}}]$$

with

$$\mathbf{U}_{s,\infty}(\hat{\mathbf{x}}) = -\frac{k_s^2}{4\,\pi\,\rho\,\omega^2} \int_{\partial D} \left\{ i\,k_s\,\mu\,[(\mathbf{u}^s \cdot \hat{\mathbf{x}})\,\mathbf{n} + (\mathbf{n} \cdot \hat{\mathbf{x}})\,\mathbf{u}^s] + \mathbf{t}^s \right\} e^{-i\,k_s\,\hat{\mathbf{x}}\cdot\mathbf{y}}\,da_{\mathbf{y}},$$

so that it is perpendicular to $\hat{\mathbf{x}}$. Thus the asymptotic expression of $\mathbf{u}^s$ results from superposition of the "outgoing spherically symmetric waves" $e^{i\,k_{p,s}\,r}/r$. The p-component of $\mathbf{u}^s$ is parallel to the ray of unit vector $\hat{\mathbf{x}}$ while the s-component is perpendicular. We conclude that the far-field pattern of the displacement vector $\mathbf{u}^s$ is given by a pair, namely

$$\mathbf{u}^s_\infty(\hat{\mathbf{x}}) = \left[\mathbf{u}^s_{p,\infty}(\hat{\mathbf{x}}), \mathbf{u}^s_{s,\infty}(\hat{\mathbf{x}})\right]. \tag{21}$$

We refer to $\mathbf{u}^s_{p,\infty}$ and $\mathbf{u}^s_{s,\infty}$ as the parallel (longitudinal) and transverse far-field patterns of $\mathbf{u}^s$, respectively[2,12,13]. Longitudinal and transverse far-field patterns for a forward scattering transmission problem in the 2D case have been examined in the literature[25].

The asymptotic expression of the stress tensor $\mathbf{T}$ associated with $\mathbf{u}^s$ is given by

$$\begin{aligned} \mathbf{T}^s(\mathbf{x}) = {} & i\,k_p\,\frac{e^{i\,k_p\,r}}{r}\left[\lambda\left(\hat{\mathbf{x}}\cdot\mathbf{u}^s_{p,\infty}\right)\,\mathbf{I} + 2\,\mu\,\hat{\mathbf{x}}\otimes\mathbf{u}^s_{p,\infty}\right] + \\ & + i\,k_s\,\mu\,\frac{e^{i\,k_s\,r}}{r}\left[\hat{\mathbf{x}}\otimes\mathbf{u}^s_{s,\infty} + \mathbf{u}^s_{s,\infty}\otimes\hat{\mathbf{x}}\right] + O\left(\frac{1}{r^2}\right), \quad \text{as } r\to\infty. \end{aligned} \tag{22}$$

For later reference, we consider the displacement $\mathbf{G}(\mathbf{x};\mathbf{z},\mathbf{q})$ identified by the unit force placed at the point $\mathbf{z}$ and acting in the direction of the unit vector $\mathbf{q}$. To simplify the notation we superpose a $\tilde{}$ to mean that dependence on the parameters $\mathbf{z}$ and $\mathbf{q}$ is omitted. For example, $\tilde{\mathbf{G}}(\mathbf{x})$ stands for $\mathbf{G}(\mathbf{x};\mathbf{z},\mathbf{q})$. The corresponding asymptotic behavior is given by

$$\tilde{\mathbf{G}}\,(r\,\hat{\mathbf{x}}) = \frac{e^{i\,k_p\,r}}{r}\left\{\tilde{\mathbf{G}}_{p,\infty}\,(\hat{\mathbf{x}}) + O\left(\frac{1}{r}\right)\right\} + \frac{e^{i\,k_s\,r}}{r}\left\{\tilde{\mathbf{G}}_{s,\infty}\,(\hat{\mathbf{x}}) + O\left(\frac{1}{r}\right)\right\},$$

where

$$\begin{aligned} \tilde{\mathbf{G}}_{p,\infty}\,(\hat{\mathbf{x}}) &= \frac{k_p^2}{4\,\pi\,\rho\,\omega^2}\,e^{-i\,k_p\,\hat{\mathbf{x}}\cdot\mathbf{z}}\;(\hat{\mathbf{x}}\cdot\mathbf{q})\;\hat{\mathbf{x}}, \\ \tilde{\mathbf{G}}_{s,\infty}\,(\hat{\mathbf{x}}) &= \frac{k_s^2}{4\,\pi\,\rho\,\omega^2}\,e^{-i\,k_s\,\hat{\mathbf{x}}\cdot\mathbf{z}}\;[\mathbf{q} - (\mathbf{q}\cdot\hat{\mathbf{x}})\;\hat{\mathbf{x}}]. \end{aligned}$$

Therefore, the far-field pattern of $\tilde{\mathbf{G}}(\mathbf{x})$ is represented by a pair,

$$\tilde{\mathbf{G}}_\infty(\hat{\mathbf{x}}) = \left[\tilde{\mathbf{G}}_{p,\infty}(\hat{\mathbf{x}}), \tilde{\mathbf{G}}_{s,\infty}(\hat{\mathbf{x}})\right].$$

To introduce the energy streamlines of $\mathbf{u}^s$, consider the equation of motion (17) written in the form

$$\nabla \cdot \mathbf{T}^s + \rho\,\omega^2\,\mathbf{u}^s = 0 \quad \text{in} \quad \mathbb{R}^3 \setminus \bar{D}.$$

Next take the scalar product with $\bar{\mathbf{u}}^s$ and subtract the equation which is obtained by interchanging $\mathbf{u}^s$ and $\bar{\mathbf{u}}^s$. The resulting equation takes the form

$$\nabla \cdot \mathbf{s} = 0 \quad \text{in} \quad \mathbb{R}^3 \setminus \bar{D}, \tag{23}$$

where the (real-valued) vector $\mathbf{s}$ is defined by

$$\mathbf{s} = \frac{\omega}{2}\,\Im\left(\mathbf{T}^s\,\bar{\mathbf{u}}^s\right) = -\frac{1}{2}\,\Re\left(\mathbf{T}^s\bar{\mathbf{v}}^s\right), \tag{24}$$

and $\mathbf{v}^s = -i\,\omega\,\mathbf{u}^s$ is the velocity. Accordingly, $\mathbf{s}$ is the mean value, over a period, of the instantaneous power-flux density vector[1,10,27]. Relation (23) is the same as (1), but, unlike the latter, it does not follow from the Helmholtz equation, thus showing that our approach, based on energy conservation along flow tubes, does not rely on this equation.

The integral curves of $\mathbf{s}$ are the energy streamlines of $\mathbf{u}^s$, and (12) holds for flow tubes, as in the case of acoustic waves. Moreover, comparison with the asymptotic expression (22) of the stress tensor $\mathbf{T}^s$ leads to

$$\mathcal{F}_{\Omega_r}[\mathbf{s}] = \frac{1}{2}\,\omega^3\,\rho\,\left[\frac{1}{k_p}\int_\Omega \left|\mathbf{u}^s_{p,\infty}\right|^2\,da + \frac{1}{k_s}\int_\Omega \left|\mathbf{u}^s_{s,\infty}\right|^2\,da\right] + O\left(\frac{1}{r}\right) \quad \text{as } r \to \infty,$$

where Ω is the unit sphere, as in the previous section. In words, the asymptotic value of the power flux is a (positive) linear superposition of the integrals over the unit sphere of the squared moduli of the parallel and the transverse far-field patterns of $\mathbf{u}^s$. It follows that

$$\lim_{r\to\infty} \mathcal{F}_{\Omega_r}[\mathbf{s}] = \frac{1}{2}\,\omega^3\,\rho\,\left[\frac{1}{k_p}\,\left\|\mathbf{u}^s_{p,\infty}\right\|^2_{L^2(\Omega)} + \frac{1}{k_s}\,\left\|\mathbf{u}^s_{s,\infty}\right\|^2_{L^2(\Omega)}\right]. \tag{25}$$

Next we consider the inverse scattering problem under the assumption that the far-field pattern is given. We follow the analogy with the previous application of the LSM in the case of acoustic waves in fluids.

As a first step we need a description of plane incident waves appropriate for the formulation of the far-field equation. Any incident harmonic plane wave propagating in the direction of the unit vector $\mathbf{d}$ may be regarded as a linear superposition of the three waves

$$\mathbf{u}^{i,1}(\mathbf{x};\mathbf{d}) = \mathbf{d}\, e^{i\,k_p\,\mathbf{d}\cdot\mathbf{x}}, \qquad \mathbf{u}^{i,2}(\mathbf{x};\mathbf{d}) = \mathbf{e}_\theta(\mathbf{d})\, e^{i\,k_s\,\mathbf{d}\cdot\mathbf{x}}, \qquad \mathbf{u}^{i,3}(\mathbf{x};\mathbf{d}) = \mathbf{e}_\phi(\mathbf{d})\, e^{i\,k_s\,\mathbf{d}\cdot\mathbf{x}}. \quad (26)$$

This follows from the properties of harmonic plane wave solutions of the Navier equation (17). The vector $\mathbf{d}$ identifies a point of the unit sphere; $\mathbf{e}_\theta(\mathbf{d})$ and $\mathbf{e}_\phi(\mathbf{d})$ denote the unit tangent vector to the meridian and the parallel through the point $\mathbf{d}$, respectively; the two vectors form the orthonormal basis tangent to the unit sphere at $\mathbf{d}$, naturally associated with the spherical coordinates (r,θ,ϕ). Of course, $\mathbf{u}^{i,1}$ is a longitudinal wave, while $\mathbf{u}^{i,2}$ and $\mathbf{u}^{i,3}$ are transverse waves.

If we denote by $\mathbf{u}^{s,j}(\mathbf{x};\mathbf{d})$ the scattered field generated by the plane incident wave $\mathbf{u}^{i,j}$, $j=1,2,3$, it follows from (21) that the corresponding far-field pattern is

$$\mathbf{u}_\infty^{s,j}(\hat{\mathbf{x}};\mathbf{d}) = \left[\mathbf{u}_{p,\infty}^{s,j}(\hat{\mathbf{x}};\mathbf{d}), \mathbf{u}_{s,\infty}^{s,j}(\hat{\mathbf{x}};\mathbf{d})\right], \qquad j=1,2,3. \quad (27)$$

We assume that the far-field pattern is given for all $\hat{\mathbf{x}},\mathbf{d}\in\Omega$. The (vector) FFE for the unknown functions $g_j(\mathbf{d};\mathbf{z},\mathbf{q}) = \tilde{g}_j(\mathbf{d})$, $j=1,2,3$, is the linear integral equation

$$\sum_{j=1}^{3}\int_\Omega \left[\mathbf{u}_{p,\infty}^{s,j}(\hat{\mathbf{x}};\mathbf{d}) + \mathbf{u}_{s,\infty}^{s,j}(\hat{\mathbf{x}};\mathbf{d})\right]\tilde{g}_j(\mathbf{d})\, da_{\mathbf{d}} = \tilde{\mathbf{G}}_{p,\infty}(\hat{\mathbf{x}}) + \tilde{\mathbf{G}}_{s,\infty}(\hat{\mathbf{x}}). \quad (28)$$

Eq. (28) can be decomposed into a radial equation (for the p-components) and two independent transverse equation (for the s-components). Eq. (28) corresponds to the (elastic) FFE considered in previous papers[2,12,13,25,26] for specific scattering conditions.

To discuss the physical content of the FFE (28), we consider the incident field defined as superposition of harmonic plane waves

$$\tilde{\mathbf{u}}^i(\mathbf{x}) = \sum_{j=1}^{3}\int_\Omega \mathbf{u}^{i,j}(\mathbf{x};\mathbf{d})\,\tilde{g}_j(\mathbf{d})\, da_{\mathbf{d}}.$$

The corresponding radiated displacement field generated by interaction with the obstacle is

$$\tilde{\mathbf{u}}^s(\mathbf{x}) = \sum_{j=1}^{3}\int_\Omega \mathbf{u}^{s,j}(\mathbf{x};\mathbf{d})\,\tilde{g}_j(\mathbf{d})\, da_{\mathbf{d}}, \quad (29)$$

with far-field pattern coinciding with the left-hand side of the FFE (28). Hence, solving (28) corresponds to finding (a superposition of incident plane waves yielding) a radiative field with the same far-field pattern as the fundamental solution with source at the sampling point $\mathbf{z}$ and sampling force $\mathbf{q}$.

Consider an ϵ-approximate solution $\tilde{\mathbf{g}}^{\epsilon}(\mathbf{d}) := \{\tilde{g}_j^{\epsilon}(\mathbf{d}),\ j = 1, 2, 3\}$ of the FFE (28), in analogy with (8), and define the displacement $\tilde{\mathbf{u}}^{s,\epsilon}(\mathbf{x})$ according to (29). The related far-field pattern $\tilde{\mathbf{u}}_{\infty}^{s,\epsilon}$ defined as in (27) has squared L^2-norm given by

$$||\tilde{\mathbf{u}}_{\infty}^{s,\epsilon}||^2_{L^2(\Omega)} = ||\tilde{\mathbf{u}}_{p,\infty}^{s,\epsilon}||^2_{L^2(\Omega)} + ||\tilde{\mathbf{u}}_{s,\infty}^{s,\epsilon}||^2_{L^2(\Omega)}.$$

Henceforth a procedure analogous to that of the previous section applies and the argument based on invariance of the power flux through sections of flow tubes leads to the blowing up of $\|\tilde{\mathbf{g}}^{\epsilon}\|_{[L^2(\Omega)]}$, as $\mathbf{z} \to \mathbf{z}^* \in \partial D$ from inside.

A number of variants of this fundamental approach can be realized. For example, suppose that the incident fields are given in the form of plane harmonic *parallel* waves described as $\mathbf{u}^{i,1}(\mathbf{x}; \mathbf{d})$ (cf. (26)). Assume that the corresponding radial far-field patterns $\mathbf{u}_{p,\infty}^{s,1}(\hat{\mathbf{x}}; \mathbf{d})$ have been measured. Consider the 'radial component' of the FFE (28), in the reduced form

$$\int_{\Omega} \mathbf{u}_{p,\infty}^{s,1}(\hat{\mathbf{x}}; \mathbf{d})\ \tilde{g}_1(\mathbf{d})\, da_{\mathbf{d}} = \tilde{\mathbf{G}}_{p,\infty}(\hat{\mathbf{x}}), \tag{30}$$

for the unknown $\tilde{g}_1 \in L^2(\Omega)$. The previous discussion then applies to the displacement field

$$\tilde{\mathbf{u}}^{s,\epsilon}(\mathbf{x}) = \int_{\Omega} \mathbf{u}^{s,1}(\mathbf{x}; \mathbf{d})\, \tilde{g}_1^{\epsilon}(\mathbf{d})\, da_{\mathbf{d}}$$

for any ϵ-approximate solution $\tilde{g}_1^{\epsilon}$ of (30), whence it follows that $\|\tilde{g}_1^{\epsilon}\|_{L^2(\Omega)}$ diverges as $\mathbf{z} \to \mathbf{z}^* \in \partial D$ or for $\mathbf{z} \notin D$. Accordingly, $||\tilde{g}_1^{\epsilon}||_{L^2(\Omega)}$ is an indicator of the boundary of the obstacle.

To illustrate another possibility, suppose that the fields $\mathbf{u}^{s,j}(\mathbf{x}; \mathbf{d})$ are given for $\mathbf{x} \in S$, where S is a closed surface surrounding ∂D. Consider an approximate solution $\tilde{\mathbf{g}}^{\epsilon}(\mathbf{d})$ to the near-field equation

$$\sum_{j=1}^{3} \int_{\Omega} \mathbf{u}^{s,j}(\mathbf{x}; \mathbf{d})\, \tilde{g}_j^{\epsilon}(\mathbf{d})\, da_{\mathbf{d}} = \tilde{\mathbf{G}}(\mathbf{x}), \qquad \mathbf{x} \in S.$$

If the power flux associated with the displacement

$$\tilde{\mathbf{u}}^{s,\epsilon}(\mathbf{x}) = \sum_{j=1}^{3} \int_{\Omega} \mathbf{u}^{s,j}(\mathbf{x};\mathbf{d})\, \tilde{g}_j^{\epsilon}(\mathbf{d})\, da_{\mathbf{d}}$$

is strictly positive at any point of S, then the previous result on the indicator property of $\tilde{\mathbf{g}}^{\epsilon}$ holds, provided that the asymptotic cross-sections of flow tubes in the far-field regions are replaced by their cross-sections on S.

IV. COMMENTS AND CONCLUSIONS

This paper provides a physical interpretation of the LSM in the case of isotropic solid matrices. The approach is inspired by (and in part borrowed from) an analogous one formulated to motivate the LSM in the case of 3D acoustic and 2D electromagnetic scattering. Conservation of energy and the property of the energy flow lines, of carrying power from the obstacle to infinity, are at the basis of this application.

The required data are given in the form of far-field patterns determined by incident harmonic plane waves, parameterized by the direction of incidence. Conservation of energy across sections of flow tubes generated by energy streamlines shows that ϵ-approximate solutions to the FFE (28) in a solid matrix act as indicators of the boundary. The results have been proved under simplifying assumptions, but more complex situations could be discussed within this framework (e.g., the case of an inhomogeneous and lossy background for 2D electromagnetic scattering problems has been investigated according to the same guidelines[3]).

This paper also suggests simplified variants of the general approach, whereby, e.g., only longitudinal incident plane waves are considered in solids and the vector FFE is replaced by its radial projection. Alternatively, the near-field equation may be considered instead of the FFE. This shows the flexibility of the LSM.

Energy streamlines suggest a physical interpretation of the LSM for inverse scattering problems, but they are not explicitly involved in the algorithm for the determination of the domain of the scatterer. We hope that this gap can be overcome in future work. Our

conjecture is that the intersection points of energy flow lines traced back from infinity are interior to the scatterer and hence provide a visualization of the interior of the unknown domain.

References

[1] Achenbach, J. D. **(1973)**. *Wave Propagation in Elastic Solids* (North-Holland, Amsterdam), Chap. 1.

[2] Alves, C. J. S., and Kress, R. **(2002)**. "On the far-field operator in elastic obstacle scattering," IMA J. Appl. Math. **67** (1), 1-21.

[3] Aramini, R., Brignone, M., Caviglia, G., Massa, A., and Piana, M. **(2011)**. "The linear sampling method in a lossy background: an energy perspective," Inverse Problems in Science and Engineering, 1-22, iFirst.

[4] Aramini, R., Caviglia, G., and Giorgi, G. **(2011)**. "The role of point sources and their power fluxes in the linear sampling method," SIAM J. Appl. Math. **71** (4), pp. 1044-1069.

[5] Aramini, R., Caviglia, G., Massa A., and Piana, M. **(2010)**. "The linear sampling method and energy conservation," Inverse Problems **26**, 055004.

[6] Arens, T. **(2004)**. "Why linear sampling works," Inverse Problems **20**, 163-173.

[7] Arens, T., and Lechleiter, A. **(2009)**. "The linear sampling method revisited," J. Integral Equations Appl. **21** (2), 179-202.

[8] Brignone, M., Bozza, G., Aramini, R., Pastorino, M., and Piana, M. **(2009)**. "A fully no-sampling formulation of the linear sampling method for three-dimensional inverse electromagnetic scattering problems," Inverse Problems **25**, 015014.

[9] Cakoni, F., and Colton, D. **(2006)**. *Qualitative Methods in Inverse Scattering Theory* (Springer, Berlin), 227 pp.

[10] Caviglia, G., and Morro, A. **(1992)**. *Inhomogeneous Waves in Solids and Fluids* (World Scientific, Singapore), Chap. 7.

[11] Chapman, D. M. F. **(2008)**. "Using streamlines to visualize acoustic energy flow across

boundaries," J. Acoust. Soc. Am. **124** (1), 48-56.

[12] Charalambopoulos, A., Gintides, D., and Kiriaki, K. **(2002)**. "The linear sampling method for the transmission problem in three-dimensional linear elasticity," Inverse Problems **18**, 547-558.

[13] Charalambopoulos, A., Gintides, D., and Kiriaki, K. **(2003)**. "The linear sampling method for non-absorbing penetrable elastic bodies," Inverse Problems **19**, 549-561.

[14] Chien, C. F., and Waterhouse, R. V. **(1997)**. "Singular points of intensity streamlines in two-dimensional sound fields," J. Acoust. Soc. Am. **101** (2), 705-712.

[15] Collino, F., Fares, M'B., and Haddar, H. **(2003)**. "Numerical and analytical studies of the linear sampling method in electromagnetic inverse scattering problems," Inverse Problems **19**, 1279-1298.

[16] Colton, D., Haddar, H., and Piana, M. **(2003)**. "The linear sampling method in inverse electromagnetic scattering theory," Inverse Problems **19**, S105-S137.

[17] Colton, D., and Kress, R. **(1998)**. *Inverse Acoustic and Electromagnetic Scattering Theory* (Springer, Berlin), Chap. 2 and 3.

[18] Colton, D., Piana, M., and Potthast, R. **(1997)**. "A simple method using Morozov's discrepancy principle for solving inverse scattering problems," Inverse Problems **13**, 1477-1493.

[19] Eringen, A. C., and Suhubi E. S. **(1975)**. *Elastodynamics, Vol. II* (Academic Press, New York), Chap. 5.

[20] Foreman, T. L. **(1989)**. "An exact ray theoretical formulation of the Helmholtz equation," J. Acoust. Soc. Am. **86** (1), 234-246.

[21] Godin, O. A. **(2009)**. "Wave refraction at an interface: Snell's law versus Chapman's law," J. Acoust. Soc. Am. **125** (4), EL117-EL122.

[22] Nintcheu Fata, S., and Guzina B. B.**(2007)**. "Elastic scatterer reconstruction via the adjoint sampling method," SIAM J. Appl. Math. **67** (5), 1330-1352.

[23] Pao, Y., and Varatharajulu, V. **(1976)**. "Huyghens' principle, radiation conditions, and integral formulas for the scattering of elastic waves," J. Acoust. Soc. Am. **59** (6), 1361-

1371.

[24] Payton, R. G. **(1983)**. *Elastic Wave Propagation in Transversely Isotropic Media* (M. Nijoff Publishers, The Hague), Chap. 1.

[25] Sevroglou, V. **(2005)**. "The far-field operator for penetrable and absorbing obstacles in 2D inverse elastic scattering," Inverse Problems **21**, 717-738.

[26] Sevroglou, V., and Pelekanos, G. **(2002)**. "Two-dimensional elastic Herglotz functions and their applications in inverse scattering," J. Elasticity **68**, 123-144.

[27] Stroh, A. N. **(1962)**. "Steady state problems in anisotropic elasticity," J. Math. Phys. **41**, 77-103.

[28] Waterhouse, R. V., Yates, T. W., Feit, D., and Liu, Y. N. **(1985)**. "Energy streamlines of a sound source," J. Acoust. Soc. Am. **78** (2), 758-762.

[29] Zhang, J., and Zhang, G. **(1990)**. "Analysis of acoustic radiation and scattering from a submerged spherical shell by energy streamlines," J. Acoust. Soc. Am. **88** (4), 1981-1985.

List of Figures